Liquid Crystals
Publication details, including instructions for authors and subscription information:
http://www.tandfonline.com/loi/tlct20

Synthesis of laterally substituted α-methylstilbene-tolane liquid crystals

Chin-Yen Chang [a] , Szu-Yuan Chien [a] , Chain-Shu Hsu [a] , Sebastian Gauza [b] & Shin-Tson Wu [b]
[a] Department of Applied Chemistry , National Chiao Tung University , Hsinchu, Taiwan 30010, ROC
[b] College of Optics and Photonics , University of Central Florida , Orlando, FL 32816, USA
Published online: 03 Jan 2008.

To cite this article: Chin-Yen Chang , Szu-Yuan Chien , Chain-Shu Hsu , Sebastian Gauza & Shin-Tson Wu (2008) Synthesis of laterally substituted α-methylstilbene-tolane liquid crystals, Liquid Crystals, 35:1, 1-9, DOI: 10.1080/02678290701743027

To link to this article: http://dx.doi.org/10.1080/02678290701743027

Liquid Crystals, Vol. 35, No. 1, January 2008, 1–9

Synthesis of laterally substituted α-methylstilbene-tolane liquid crystals

CHIN-YEN CHANG†, SZU-YUAN CHIEN†, CHAIN-SHU HSU*†, SEBASTIAN GAUZA‡ and SHIN-TSON WU‡

†Department of Applied Chemistry, National Chiao Tung University, Hsinchu, Taiwan 30010, ROC
‡College of Optics and Photonics, University of Central Florida, Orlando, FL 32816, USA

(*Received 4 July 2007; accepted 3 October 2007*)

Three series of α-methylstilbene-tolane liquid crystals, 4-[2-(4-alkylphenyl)-1-ethynyl]-4′-fluoro-α-methylstilbene (**3a**–**3e**), 4-[2-(4-alkylphenyl)-1-ethynyl]-2′-methyl-4′-fluoro-α-methylstilbene (**4a**–**4e**) and 4-[2-(4-alkylphenyl)-1-ethynyl]-3′-methyl-4′-fluoro-α-methylstilbene (**5a**–**5e**), were synthesized and their phase transition temperatures characterized. All the α-methylstilbene-tolane liquid crystals exhibit an enantiotropic nematic phase. Compounds **5a**–**5e**, which contain a lateral methyl group at the 3 position of the middle phenyl ring, display low melting points, a wide nematic range and a small enthalpy of fusion. Their potential applications for displays and laser-beam steering are noted.

1. Introduction

High birefringence (Δn) liquid crystals are attractive materials for applications in reflective liquid crystal displays (LCDs) [1], infrared spatial light modulators [2], polymer-dispersed liquid crystals (PDLCs) [3], cholesteric LCDs (Ch-LCDs) [4], holographic switching devices [5], polarizers and directional reflectors [6, 7] and laser beam steering [8]. In PDLCs and Ch-LCDs, high Δn improves display brightness and contrast ratio. In addition, high Δn and low viscosity compounds are particularly essential for colour sequential displays.

It is well known that a high Δn value can be achieved by increasing the molecular conjugation length [9]. Several molecular structures with high Δn values, e.g. diphenyldiacetylene [10–12], biphenyltolane [13], bistolane [14, 15], naphthalene tolanes [16], naphthylbistolanes [17] and thiophenylacetylene [18, 19] have be widely studied. However, a general problem for these highly conjugated molecules is their high melting points. Some symmetric bistolanes have been reported in the literature [20–23], but their melting points are extraordinarily high (>200°C). How to lower the melting temperatures of these compounds is a major challenge. The general approach is to introduce a lateral fluoro or alkyl group onto the mesogenic core to lower the melting points of tolane and bistolane liquid crystals [23–29]. Recently, Spells *et al.* [30] reported the synthesis of fluorinated stilbene-tolane liquid crystals, but their melting points were higher than 220°C.

In this paper, we report the synthesis of three series of fluorinated α-methylstilbene-tolane compounds. We introduced the α-methylstilbene group and lateral methyl substituent to lower the melting point. The mesomorphic properties as well as optical anisotropies of the synthesized liquid crystals are discussed. The general chemical structure of the compounds studied is shown in figure 1. In this study, *n* was limited to 2–6 for low viscosity considerations.

2. Experimental

2.1. *Materials*

4-Fluoro-α-methylstyrene, 4-bromoaniline, 4-bromo-2-methylaniline, 4-bromo-3-methylaniline, palladium acetate, tri-*o*-tolylphosphine and other reagents were purchased from Aldrich and used as received. Dichloromethane and triethylamine were dried over CaH_2, tetrahydrofuran was dried over $LiAlH_4$ and distilled before use.

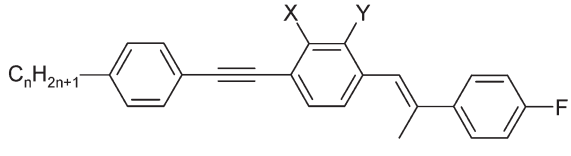

n = 2–6; X and Y = H or CH_3

Figure 1. Structure of the α-methylstilbene-tolane materials studied.

*Corresponding author. Email: cshsu@mail.nctu.edu.tw

Liquid Crystals
ISSN 0267-8292 print/ISSN 1366-5855 online © 2008 Taylor & Francis
http://www.tandf.co.uk/journals
DOI: 10.1080/02678290701743027

4-*n*-Alkylphenylacetylenes were synthesized according to the method described by Li and Wen [29].

2.2. *Characterization techniques*

^{1}H NMR spectra (300 MHz) were recorded on Varian VXR-300 spectrometer. Thermal transitions and thermodynamic parameters were determined by using a Seiko SSC/6200 differential scanning calorimeter equipped with a liquid nitrogen cooling accessory. Heating and cooling rates were 1°C min^{-1}. Transition temperatures reported here were collected during the second heating and first cooling scans. A Carl Zeiss Axiphot polarizing optical microscope equipped with a Mettler FP 82 hot stage and a FP 80 central processor was used to observe the thermal transitions and analyse the anisotropic textures.

2.3. *Synthesis of fluorinated α-methylstilbene-tolanes*

Scheme 1 illustrates the procedure used to synthesize the fluorinated α-methylstilbene-tolane compounds.

2.3.1. 4-Fluoro-4′-iodo-α-methylstilbene, 4′-fluoro-4-iodo-2′-methyl-α-methylstilbene and 4-fluoro-4′-iodo-3′-methyl-α-methyllstilbene (2a–2c) [24, 28]. Compounds **2a**–**2c** were prepared by analogous methods. The synthesis of compound **2a** is described below.

4-Fluoro-α-methylstyrene (1.63 g, 0.012 mmol), 4-bromoaniline (1.72 g, 10 mmol), palladium(II) acetate (22.4 mg, 0.1 mmol), and tri-*o*-tolylphosphine (91.2 mg, 0.3 mmol) were dissolved in a mixed solvent of triethylamine (9 ml) and acetonitrile (4 ml). The reaction mixture was stirred at 100°C for 48 h under nitrogen atmosphere. After cooling to room temperature, the solution was concentrated by a rotary evaporator, and the residue was dissolved in 100 ml of diethyl ether. The diethyl ether solution was washed with water and dried over anhydrous $MgSO_4$. After the solvent was removed the crude product **1a** was isolated.

The crude product **1a** was redissolved in THF (30 ml) and cooled to 0°C. A mixture of concentrated HCl (2.5 ml) and aqueous sodium nitrite (2.07 g in 7 ml of H_2O) aqueous solution was added. The reaction mixture was stirred at 0°C for 10 min and then treated with KI (5 g in 5 ml of H_2O) aqueous solution. The mixture was stirred at 0°C for 3 h, and 50 ml of saturated sodium thiosulfate aqueous solution was added. The reaction mixture was extracted with ethyl acetate. The collected organic layer was washed with brine and water, and dried over anhydrous $MgSO_4$. After the solvent was removed, the crude product was purified by column chromatography (silica gel, hexane as eluent) to yield 2.2 g (54%) of white crystals, m.p. = 94.5°C.

For **2a**, ^{1}H NMR ($CDCl_3$): δ2.23 (s, 3H, Ph(C**H**$_3$)C=CHPh), 6.78 (s, 1H, Ph(CH$_3$)C=C**H**Ph), 7.00–7.06 (t, 2 aromatic protons), 7.36–7.39 (d, 2 aromatic protons), 7.46–7.49 (d, 2 aromatic protons), 7.68–7.70 (d, 2 aromatic protons).

For **2b**, yield 38%. ^{1}H NMR ($CDCl_3$): δ2.04 (s, 3H, Ph-C**H**$_3$), 2.21 (s, 1H, Ph(C**H**$_3$)C=CHPh), 6.63 (s, 3H, Ph(CH$_3$)C=C**H**Ph), 6.91–6.94 (d, 1 aromatic proton), 7.00–7.06 (t, 2 aromatic protons), 7.38–7.50 (m, 4 aromatic protons), colourless oil.

For **2c**, yield 53%. ^{1}H NMR ($CDCl_3$): δ2.43 (s, 3H, PhC**H**$_3$), 2.23 (s, 1H, Ph(C**H**$_3$)C=CHPh), 6.63 (s, 3H, Ph(CH$_3$)C=C**H**Ph), 6.91 (s, 1H, aromatic proton), 7.00–7.06 (t, 2 aromatic protons), 7.14–7.18 (d, 1 aromatic proton), 7.42–7.48 (d, 2 aromatic protons), 7.75–7.78 (d, 1 aromatic proton), colourless oil.

2.3.2. 4-[2-(4-Alkylphenyl)-1-ethynyl]-4′-fluoro-α-methylstilbene (3a–3e), 4-[2-(4-alkylphenyl)-1-ethynyl]-2′-methyl-4′-fluoro-α-methylstilbene (4a–4e) and 4-[2-(4-alkylphenyl)-1-ethynyl]-3′-methyl-4′-fluoro-α-methylstilbene (5a–5e). All the compounds, **3a**–**3e**, **4a**–**4e** and **5a**–**5e**, were prepared by Cadiot–Chodkiewicz coupling [25] of a 4-alkylphenylacetylene with compounds **2a**–**2c**, respectively. The compounds were purified several times by column chromatography until purities were higher than 99%. The synthesis of compound **3a** is described below.

4-Ethylphenylacetylene (0.13 g, 1.00 mmol), 4-fluoro-4′-iodo-α-methylstilbene (0.34 g, 1.00 mmol), triphenylphosphine (13 mg, 0.05 mmol), copper iodide (2 mg, 0.01 mmol) and bis(triphenylphosphine)palladium dichloride (7 mg, 0.01 mmol) were dissolved in 10 ml of triethylamine. The reaction mixture was stirred at 40°C for 5 h. After the solvent was removed under vacuum, the residue was dissolved in 30 ml of dichloromethane. The dichloromethane solution was washed three times with 10% HCl aqueous solution and water. The organic layer was dried over anhydrous $MgSO_4$ and again concentrated by rotary evaporation. The resulting solid was recrystallized from chloroform to yield 0.32 g (95%) of light yellow crystals.

For **3a**, IR (KBr) ν_{max}/cm^{-1}: 3028, 2950, 2929, 2859, 1599, 1508, 1234, 837. ^{1}H NMR($CDCl_3$): δ 1.15–1.20 (t, 3H, –CH$_3$), 2.21 (s, 3H, Ph(C**H**$_3$)C=CHPh), 2.59–2.67 (q, 2H, PhC**H**$_2$CH$_3$), 6.69 (s, 1H, PhC(CH$_3$)=C**H**Ph), 7.03–7.08 (t, 2 aromatic protons), 7.15–7.18 (d, 2 aromatic protons), 7.32–7.35 (d, 2 aromatic protons), 7.44–7.54 (m, 6 aromatic protons). HRMS: *m*/*z* calculated for $C_{25}H_{21}F$, 382.2097; found 382.2091. Elemental analysis: calculated for $C_{25}H_{21}F$, C 88.2, H 6.22; found C 88.24, H, 6.42%.

For **3b**, yield 94%. ^{1}H NMR ($CDCl_3$): δ 0.92–0.97 (t, 3H, CH$_3$), 1.62–1.69 (m, 2H, –C**H**$_2$CH$_3$), 2.28 (s, 3H,

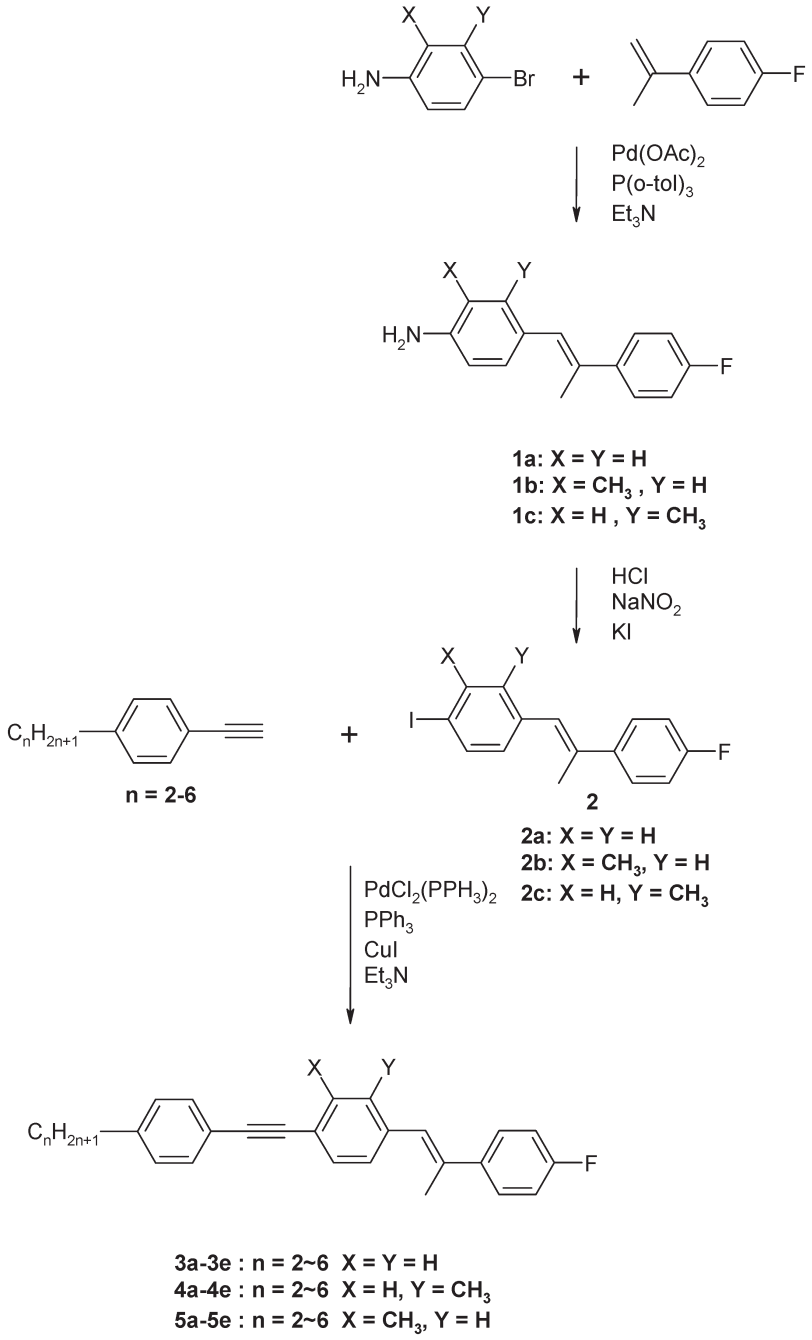

Scheme 1: Synthesis of α-methylstilbene-tolane liquid crystals.

Ph(C**H**$_3$)C=CHPh), 2.58–2.63 (t, 2H, PhC**H**$_2$–), 6.76 (s, 1H, Ph(CH$_3$)C=C**H**Ph), 7.03–7.09 (t, 2 aromatic protons), 7.15–7.18 (d, 2 aromatic protons), 7.32–7.35 (d, 2 aromatic protons), 7.44–7.54 (m, 6 aromatic protons). HRMS: *m*/*z* calculated for $C_{26}H_{23}F$, 396.2253; found 396.2251. Elemental analysis: calculated for $C_{26}H_{23}F$, C 88.1, H 6.54; found C 88.09, H 6.53%.

For **3c**, yield 95%. ^{1}H NMR ($CDCl_3$): δ 0.91–0.96 (t, 3H, –CH$_3$), 1.32–1.40 (m, 2H, –C**H**$_2$CH$_3$), 1.56–1.66 (m, 2H, PhCH$_2$C**H**$_2$–), 2.28 (s, 3H, Ph(C**H**$_3$)C=CHPh), 2.60–2.65 (t, 2H, PhC**H**$_2$–), 6.76 (s, 1H, Ph(CH$_3$)C=C**H**Ph), 7.03–7.09 (t, 2 aromatic protons), 7.15–7.18 (d, 2 aromatic protons), 7.32–7.35 (d, 2 aromatic protons), 7.44–7.54 (m, 6 aromatic protons). Elemental analysis: calculated for $C_{27}H_{25}F$, C 88.01, H, 6.84; found C 88.11, H 6.84%.

For **3d**, yield 95%. ^{1}H NMR ($CDCl_3$): δ 0.87–0.92 (t, 3H, –CH$_3$), 1.31–1.35 (m, 4H, –(C**H**$_2$)$_2$CH$_3$), 1.57–1.62

(m, 2H, $PhCH_2CH_2$–), 2.28 (s, 3H, $Ph(CH_3)C=CHPh$), 2.57–2.62 (t, 2H, $PhCH_2$–), 6.76 (s, 1H, $Ph(CH_3)C=CHPh$), 7.03–7.09 (t, 2 aromatic protons), 7.15–7.18 (d, 2 aromatic protons), 7.44–7.54 (m, 6 aromatic protons). Elemental analysis: calculated for $C_{28}H_{27}F$, C 87.92, H 7.11; found C 87.91, H 7.16%.

For **3e**, yield 95%. ^{1}H NMR ($CDCl_3$): δ 0.85–0.91 (t, 3H, $-CH_3$), 1.28–1.32 (m, 6H, $-(CH_2)_3CH_3$), 1.57–1.63 (m, 2H, $PhCH_2CH_2$–), 2.28 (s, 3H, $Ph(CH_3)C=CHPh$), 2.60–2.64 (t, 2H, $PhCH_2$–), 6.75 (s, 1H, $Ph(CH_3)C=CHPh$), 7.03–7.09 (t, 2 aromatic protons), 7.15–7.18 (d, 2 aromatic protons), 7.32–7.35 (d, 2 aromatic protons), 7.44–7.54 (m, 6 aromatic protons). Elemental analysis: calculated for $C_{29}H_{29}F$, C 87.84, H 7.37; found C 87.6, H 7.35%.

For **4a**, yield 93%. IR (KBr) ν_{max}/cm^{-1}: 3026, 2959, 2930, 2872, 1596, 1508, 1230, 828. ^{1}H NMR ($CDCl_3$): δ 1.20–1.25 (t, 3H, –CH3), 2.09 (s, 3H, $PhCH_3$), 2.27 (s, 3H, $Ph(CH_3)C=CHPh$), 2.60–2.69 (t, 2H, $PhCH_2$–), 6.74 (s, 1H, $Ph(CH_3)C=CHPh$), 7.05–7.15 (t, 2 aromatic protons), 7.20–7.34 (m, 3 aromatic protons), 7.36–7.51 (m, 6 aromatic protons). HRMS: *m*/*z* calculated for $C_{26}H_{23}F$, 354.1794; found 354.1800. Elemental analysis: calculated for $C_{26}H_{23}F$, C 88.10, H 6.54; found C 88.11, H 6.93%.

For **4b**, yield 95%. ^{1}H NMR ($CDCl_3$): δ 0.90–0.96 (t, 3H, $-CH_3$), 1.59–1.67 (m, 2H, $-CH_2CH_3$), 2.09 (s, 3H, $PhCH_3$), 2.27 (s, 3H, $Ph(CH_3)C=CHPh$), 2.56–2.61 (t, 2H, $PhCH_2$–), 6.74 (s, 1H, $Ph(CH_3)C=CHPh$), 7.05–7.15 (t, 2 aromatic protons), 7.20–7.34 (m, 3 aromatic protons), 7.36–7.51 (m, 6 aromatic protons). HRMS: *m*/*z* calculated for $C_{27}H_{25}F$, 368.1940; found 368.1947. Elemental analysis: calculated for $C_{27}H_{25}F$, C 88.01, H 6.84; found C 87.93, H 7.17%.

For **4c**, yield 95%. ^{1}H NMR ($CDCl_3$): δ 0.86–0.94 (t, 3H, $-CH_3$), 1.24–1.38 (m, 2H, $-CH_2CH_3$), 1.53–1.61 (m, 2H, $PhCH_2CH_2$–), 2.09 (s, 3H, $PhCH_3$), 2.27 (s, 3H, $Ph(CH_3)C=CHPh$), 2.58–2.63 (t, 2H, $PhCH_2$–), 6.74 (s, 1H, $Ph(CH_3)C=CHPh$), 7.05–7.15 (t, 2 aromatic protons), 7.20–7.34 (m, 3 aromatic protons), 7.36–7.51 (m, 6 aromatic protons). HRMS: *m*/*z* calculated for $C_{28}H_{27}F$, 382.2087; found 382.2079. Elemental analysis: calculated for $C_{28}H_{27}F$, C 87.92, H 7.11; found C 87.90, H 7.28%.

For **4d**, yield 94%. ^{1}H NMR ($CDCl_3$): δ 0.85–0.90 (t, 3H, $-CH_3$), 1.28–1.33 (m, 4H, $-(CH_2)_2CH_3$), 1.53–1.62 (m, 2H, $PhCH_2CH_2$–), 2.09 (s, 3H, $PhCH_3$), 2.27 (s, 3H, $Ph(CH_3)C=CHPh$), 2.57–2.62 (t, 2H, $PhCH_2$–), 6.74 (s, 1H, $Ph(CH_3)C=CHPh$), 7.05–7.15 (t, 2 aromatic protons), 7.20–7.34 (m, 3 aromatic protons), 7.36–7.51 (m, 6 aromatic protons). HRMS: *m*/*z* calculated for $C_{29}H_{29}F$, 396.2231; found 396.2222. Elemental analysis: calculated for $C_{29}H_{29}F$, C 87.84, H 7.37; found C 87.69, H 7.58%.

For **4e**, yield 96%. ^{1}H NMR ($CDCl_3$): δ 0.84–0.87 (t, 3H, $-CH_3$), 1.24–1.29 (m, 6H, $-(CH_2)_3CH_3$), 1.55–1.59 (m, 2H, $PhCH_2CH_2$–), 2.09 (s, 3H, $PhCH_3$), 2.27 (s, 3H, $Ph(CH_3)C=CHPh$), 2.57–2.62 (t, 2H, $PhCH_2$–), 6.74 (s, 1H, $Ph(CH_3)C=CHPh$), 7.05–7.15 (t, 2 aromatic protons), 7.20–7.34 (m, 3 aromatic protons), 7.36–7.51 (m, 6 aromatic protons). HRMS: *m*/*z* calculated for $C_{30}H_{31}F$, 410.2380; found 410.2377. Elemental analysis: calculated for $C_{30}H_{31}F$, C 87.76, H 7.61; found C 87.65, H 7.77%.

For **5a**, yield 95%. IR (KBr) ν_{max}/cm^{-1}: 3028, 2952, 2929, 2856, 1597, 1507, 1233, 836. ^{1}H NMR ($CDCl_3$): δ 1.20–1.26 (t, 3H, –CH3), 2.26 (s, 3H, Ph(CH3)C=CHPh), 2.51 (s, 3H, $PhCH_3$), 2.59–2.68 (q, 2H, $PhCH_2$–), 6.71 (s, 1H, $Ph(CH_3)C=CHPh$), 7.01–7.06 (t, 2 aromatic protons), 7.14–7.20 (m, 4 aromatic protons), 7.43–7.48 (m, 5 aromatic protons). HRMS: *m*/*z* calculated for $C_{26}H_{23}F$, 354.1783; found 354.1773. Elemental analysis: calculated for $C_{26}H_{23}F$, C 88.10, H 6.54; found C 88.14, H 6.71%.

For **5b**, yield 94%. ^{1}H NMR: δ 0.90–0.95 (t, 3H, –CH3), 1.60–1.67 (m, 2H, $-CH_2CH3$), 2.26 (s, 3H, $Ph(CH_3)C=CHPh$), 2.51 (s, 3H, $PhCH_3$), 2.56–2.61 (t, 2H, $PhCH_2$–), 6.71 (s, 1H, $Ph(CH_3)C=CHPh$), 7.01–7.06 (t, 2 aromatic protons), 7.14–7.20 (m, 4 aromatic protons), 7.43–7.48 (m, 5 aromatic protons). HRMS: *m*/*z* calculated for $C_{27}H_{25}F$, 368.1943; found 368.1952. Elemental analysis: calculated for $C_{27}H_{25}F$, C 88.01, H 6.84; found C 87.07, H 7.02%.

For **5c**, yield 95%. ^{1}H NMR ($CDCl_3$): δ 0.89–0.94 (t, 3H, –CH3), 1.32–1.37 (m, 2H, $-CH_2CH_3$), 1.52–1.62 (m, 2H, $PhCH_2CH_2$–), 2.26 (s, 3H, $Ph(CH_3)C=CHPh$), 2.51 (s, 3H, $PhCH_3$), 2.58–2.63 (t, 2H, $PhCH_2$–), 6.71 (s, 1H, $Ph(CH_3)C=CHPh$), 7.01–7.06 (t, 2 aromatic protons), 7.14–7.20 (m, 4 aromatic protons), 7.43–7.48 (m, 5 aromatic protons). HRMS: *m*/*z* calculated for $C_{28}H_{27}F$, 282.2097; found 282.2089. Elemental analysis: calculated for $C_{28}H_{27}F$, C 87.92, H 7.11; found: C 87.89, H 7.25%.

For **5d**, yield 96%. ^{1}H NMR ($CDCl_3$): δ 0.85–0.90 (t, 3H, –CH3), 1.29–1.33 (m, 2H, $-(CH_2)_2CH_3$), 1.58–1.63 (m, 2H, $PhCH_2CH_2$–), 2.26 (s, 3H, $Ph(CH_3)C=CHPh$), 2.51 (s, 3H, $PhCH_3$), 2.57–2.63(t, 2H, $PhCH_2$–), 6.71 (s, 1H, $Ph(CH_3)C=CHPh$), 7.01–7.06 (t, 2 aromatic protons), 7.14–7.20 (m, 4 aromatic protons), 7.43–7.48 (m, 5 aromatic protons). HRMS: *m*/*z* calculated for $C_{29}H_{29}F$, 396.2274; found 396.2283. Elemental analysis: calculated for $C_{29}H_{29}F$, C 87.84, H 7.37; found C 87.81, H 7.49%.

For **5e**, yield 96%. ^{1}H NMR ($CDCl_3$): δ 0.85–0.89 (t, 3H, –CH3), 1.28–1.30 (m, 6H, $-(CH_2)_3CH_3$), 1.51–1.60 (m, 2H, $PhCH_2CH_2$–), 2.26 (s, 3H, $Ph(CH_3)C=CHPh$), 2.51 (s, 3H, $PhCH_3$), 2.58–2.63 (t, 2H, $PhCH_2$–), 6.71 (s,

1H, Ph(CH_3)C=C**H**Ph), 7.01–7.06 (t, 2 aromatic protons), 7.14–7.20 (m, 4 aromatic protons), 7.43–7.48 (m, 5 aromatic protons). HRMS: *m/z* calculated for $C_{30}H_{31}F$, 410.2410; found 410.2421. Elemental analysis: calculated for $C_{30}H_{31}F$, C 87.76, H 7.61; found C 87.77, H 7.76%.

3. Results and discussion

3.1. *Effect of terminal alkyl chain*

The phase transition temperatures and corresponding enthalpy changes for compounds **3a**–**3e**, **4a**–**4e** and **5a**–**5e** are listed in table 1. All the compounds exhibit an enantiotropic nematic phase. Figure 2 shows a typical nematic texture exhibited by compound **5d**.

Compounds **3a**–**3e** posses the same mesogenic core; the only difference is the length of the terminal alkyl groups at each end. On going from **3a** to **3e**, the terminal alkyl chain length increases from ethyl to hexyl. Figure 3 shows a plot of phase transition temperatures versus the carbon number (*n*) of the alkyl group. Both melting and clearing temperatures decrease gradually with increasing carbon number of the terminal alkyl chain. This series of compounds exhibits high melting temperatures ranging from 126.3 to 165.8°C and high clearing temperature ranging from 193.6 to 217.0°C. Each compound also gives a very wide temperature range (>49.2°C) for the nematic phase.

Compounds **4a**–**4e** possess the same mesogenic core with a lateral methyl group on the 2-position of

Table 1. Phase transition temperatures (°C) and associated enthalpy data (kcal mol^{-1}, in parentheses) for the α-methylstilbene-tolane materials.

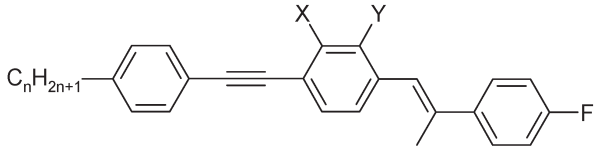

Compound	*n*	X	Y	Heating/cooling	Range/°C
3a	2	H	H	Cr 165.8 (2.16) N 215 (0.06) I I 213.5 (−0.06) N 141.0 (−2.17) Cr	49.2
3b	3	H	H	Cr 148.0 (5.18) N 217 (0.15) I I 215.7 (−0.16) N 129.0 (−5.13) Cr	69
3c	4	H	H	Cr 140.0 (5.74)) N 207.6 (0.19) I I 207.8 (−0.12) N 125.0 (−5.75) Cr	67.6
3d	5	H	H	Cr 129.7 (7.43) N 202.2 (0.14) I I 200.8 (−0.18) N 119.1 (−4.65) Cr	72.5
3e	6	H	H	Cr 126.3 (5.12) N 193.6 (0.13) I I 192.3 (−0.13) N 122.5 (−4.26) Cr	67.3
4a	2	CH_3	H	Cr 86.9 (4.35) N 147.3 (0.11) I I 145.9 (−0.17) N 50.7 (−2.77) Cr	60.4
4b	3	CH_3	H	Cr 78.5 (4.2) N 151.8 (0.09) I I 149.5 (−0.1) N 44.8 (−2.87) Cr	73.3
4c	4	CH_3	H	Cr 63.9 (4.37) N 116.2 (0.04) I I 120.2 (−0.14) N<−50 Cr	52.3
4d	5	CH_3	H	Cr 64.2 (4.97) N 120.2 (0.06) I I 123.0 (−0.16) N<−50 Cr	56
4e	6	CH_3	H	Cr 55 (3.81) N 115.1 (0.09) I I 114.4 (−0.21) N<−50 Cr	60.1
5a	2	H	CH_3	Cr 90.4 (6.15) N 183.2 (0.22) I I 177.8 (−0.24) N 52.7 (−5.57) Cr	92.8
5b	3	H	CH_3	Cr 90.2 (7.01) N 184.3 (0.33) I I 182.4 (−0.24) N 42.0 (−5.41) Cr	94.1
5c	4	H	CH_3	Cr 55 (3.81) N 115.1 (0.09) I I 114.4 (−0.21) N<−50 Cr	100.7
5d	5	H	CH_3	Cr 55 (3.81) N 115.1 (0.09) I I 114.4 (−0.21) N<−50 Cr	109.8
5e	6	H	CH_3	Cr 90.4 (6.15) N 183.2 (−0.22) I I 177.8 (−0.24) N 52.7 (−5.57) Cr	95.6

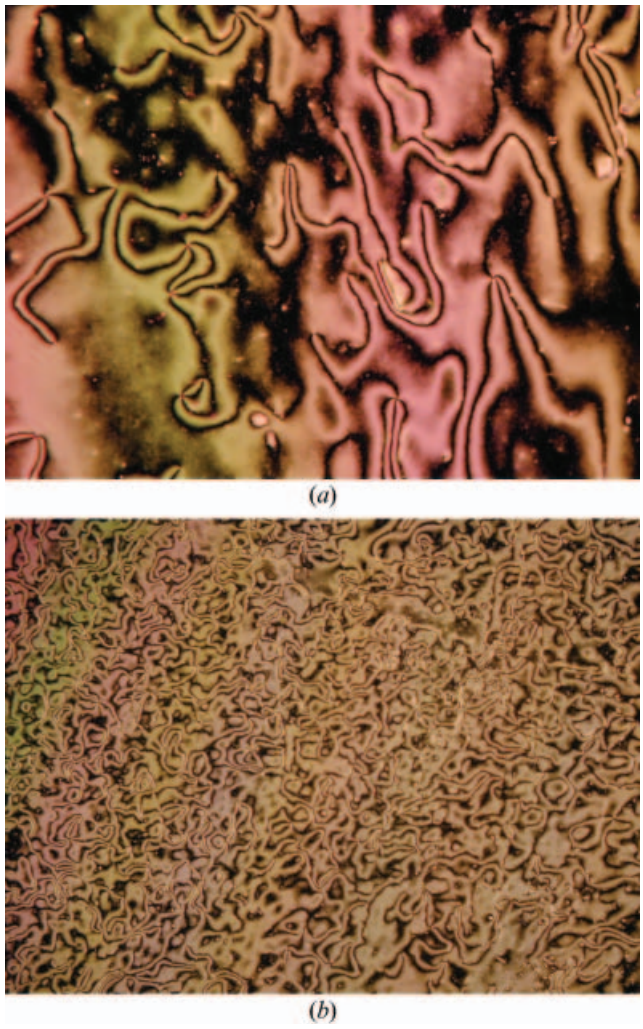

Figure 2. Optical texture of the nematic phase (a) on heating at 100°C (300 ×) and (b) on cooling at 25°C for compound **5d** (50 ×).

the middle phenyl ring. On going from **4a** to **4e**, the terminal alkyl chain length increases from ethyl to hexyl. Figure 4 shows a plot of the phase transition temperatures versus carbon number (n) of the terminal alkyl chain. As shown in figure 3, the melting points decrease gradually with increasing alkyl chain length and the isotropization temperature shows an odd–even effect with increasing alkyl chain length.

For compounds **5a**–**5e**, which contain a lateral methyl group on the 3-position of the middle phenyl ring in the mesogen, phase transition temperatures are plotted against carbon number (n) of the terminal alkyl group in figure 5. Both melting and clearing temperatures decrease with increasing carbon number of the terminal alkyl group.

3.2. *Effect of α-methyl group in stilbene unit*

In 2002, Spells *et al.* reported the synthesis and characterization of the fluorinated stilbene-tolane liquid crystals [30]. If we compare the chemical structures of our compounds **3a**–**3e** with those of their compounds **4a**–**4e**, the only difference is the α-methyl group in the stilbene unit. However, the compounds **3a**–**3e** exhibit at least a 60°C lower melting point, a 40°C lower clearing temperature and a 20°C wider nematic range. The results demonstrate that introducing the α-methyl group onto the stilbene unit can dramatically decrease the melting points of the synthesized liquid crystals.

3.3. *Effect of lateral methyl group*

In a previous study [25], we showed that the introduction of a lateral methyl group on the middle phenyl ring of bistolane compounds could dramatically decrease their phase transition temperatures. A similar phenomenon was observed for compounds **4a**–**4e** and **5a**–**5e**. According to the data listed in table 1, homologues **4a**–**4e** exhibit much lower melting temperatures (from 55.0 to 86.6°C) and clearing temperatures (from 115.1 to 147.3°C) in comparison with those of compounds **3a**–**3e**. This is because the lateral methyl group increases the molecular width, which, in turn, decreases the packing density of the liquid crystal molecules. As a result, the temperatures required to melt the crystals and to clear the liquid crystal phase are much lower. Homologues **5a**–**5e** also exhibit much lower melting temperatures ranging from 56.1 to 90.4°C, which are very close to those of compounds **4a**–**4e**. However, their clearing points do not decrease as much as those of homologues **3a**–**3e**. This indicates that homologues **5a**–**5e** exhibit a much wider nematic temperature range (>92.8°C). Figure 2 shows the typical nematic texture for compound **5d** on heating at 100°C and cooling at 25°C. In the cooling process, the solidification temperature was found to be below −50°C. This result shows that the position of the lateral methyl group also plays an important role in tuning the mesomorphic temperature range.

Some homologues (e.g. compounds **5d** and **5e**) exhibit particularly low melting points (<58°C), small fusion enthalpies (<7.8 kJ mol^{-1}) and a wide nematic range (>90°C). As a result, they are useful for formulating eutectic mixtures with a wide nematic range. The Δn values of **5d** and **5e** are estimated to be around 0.4 in the visible spectral region according to our previous reports [12, 13].

4. Conclusion

Three series of α-methylstilbene-tolane liquid crystals have been synthesized and their phase transition

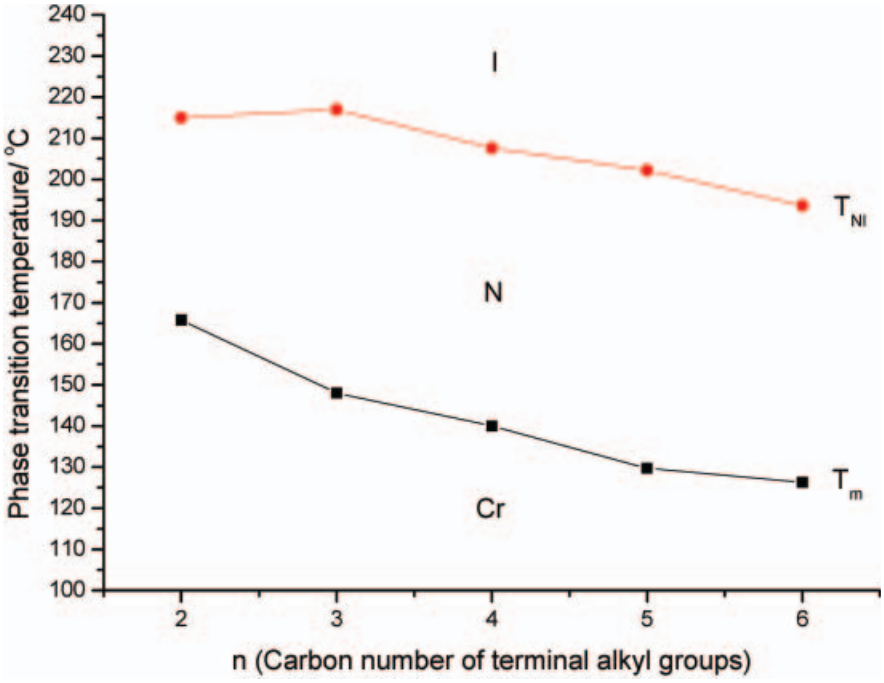

Figure 3. Melting (T_m, ■) and isotropization (T_{NI}, ●) temperatures of **3a**–**3e** as a function of the carbon number (n) of the alkyl group.

temperatures characterized. All the synthesized α-methylstilbene-tolane compounds display an enantiotropic nematic phase. The terminal alkyl groups have a profound effect on the phase transition temperatures of the α-methylstilbene-tolane; both melting and clearing temperatures decrease as the alkyl chain length

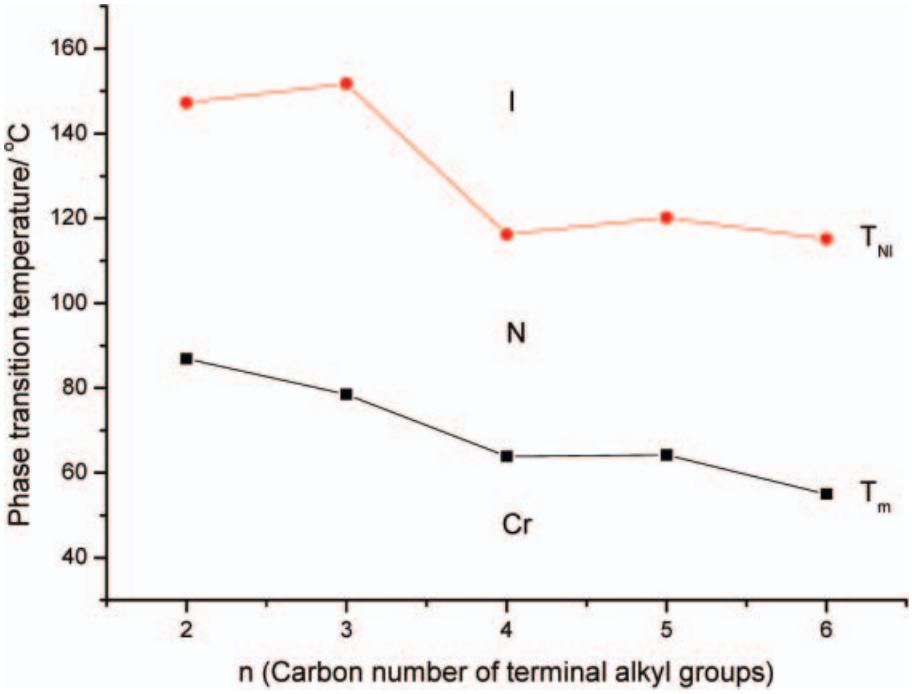

Figure 4. Melting (T_m, ■) and isotropization (T_{NI}, ●) temperatures of **4a**–**4e** as a function of the carbon number (n) of the alkyl group.

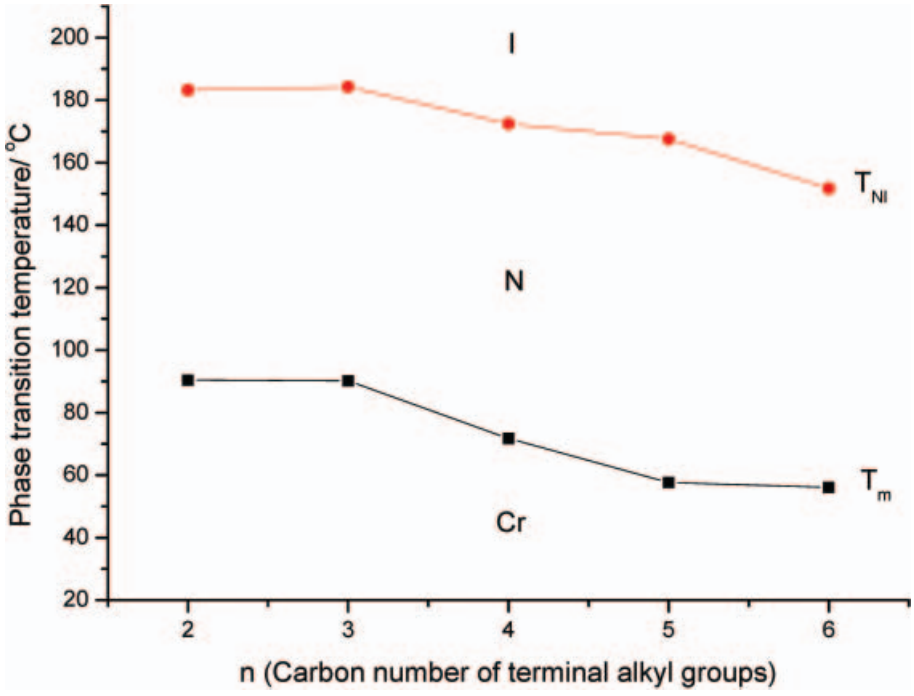

Figure 5. Melting (T_m, ■) and isotropization (T_{NI}, ●) temperatures of **5a**–**5e** as a function of the carbon number (n) of the alkyl group.

increases. The lateral methyl group plays an important role in lowering the melting temperature. Some homologues possess low melting points and high clearing temperatures and small enthalpies of fusion. These α-methylstilbene-tolane liquid crystals could find useful application in PDLC displays, reflective displays employing cholesteric liquid crystals and laser beam steering employing liquid crystal-based optical phase arrays.

Acknowledgement

The authors are grateful to the National Science Council of the Republic of China for financial support of this work.

References

[1] J.L. Fergason. *SID Dig. '86*, 68 (1986).
[2] S.T. Wu, U. Efron, J. Grinberg, L.D. Hess. *SID Tech. Dig.*, **16**, 262 (1985).
[3] J.W. Doane, N.A. Vaz, B.G. Wu, S. Zumer. *Appl. Phys. Lett.*, **48**, 269 (1986).
[4] J. Li, C. Hoke, D.S. Fredly, P.J. Bos. *SID Symp. Dig.*, **96**, 265 (1996).
[5] R.L. Sutherland, L.V. Natarajan, V.P. Tondiglia, T. Bunning. *J. Chem. Mater.*, **5**, 1533 (1993).
[6] C.C. Bowley, H. Yuan, G.P. Crawford. *Mol. Cryst. liq. Cryst.*, **331**, 209 (1999).
[7] T. Tokumaru, K. Iwauchi, Y. Higashigayi, M. Matsuura. In *Proceedings of the Anglo-Japanese Seminar on Liquid Crystals*, p. 72 (1999).
[8] P.F. Mcmanamon, E.A. Watson, T.A. Dorschner, L.J. Barnes. *Opt. Engng*, **32**, 2657 (1993).
[9] S.T. Wu. *Mol. Cryst. liq. Cryst.*, **261**, 79 (1995).
[10] S.T. Wu, J.D. Margerum, B. Meng, L.R. Dalton, C.S. Hsu, S.H. Lung. *Appl. Phys. Lett.*, **61**, 630 (1992).
[11] S.T. Wu, M. Neubert, S.S. Keast, D.G. Abdallah, S.N. Lee, M.E. Walsh, T.A. Dorschner. *Appl. Phys. Lett.*, **77**, 957 (2000).
[12] T.M. Juang, Y.N. Chen, S.H. Lung, Y.H. Lu, C.S. Hsu, S.T. Wu. *Liq. Cryst.*, **15**, 529 (1993).
[13] Y.M. Liao, N. Janarthanan, C.S. Hsu, S. Gauza, S.T. Wu. *Liq. Cryst.*, **33**, 1199 (2006).
[14] C. Sekine, N. Konya, M. Minai, K. Fujisawa. *Liq. Cryst.*, **28**, 1495 (2001).
[15] S.T. Wu, C.S. Hsu, K.F. Shyu. *Appl. Phys. Lett.*, **74**, 344 (1999).
[16] A.J. Seed, K.J. Toyne, J.W. Goodby, M. Hird. *J. Mater. Chem.*, **10**, 2096 (2000).
[17] Y.M. Liao, H.L. Chen, C.S. Hsu, S. Gauza, S.T. Wu. *Liq. Cryst.*, **34**, 507 (2007).
[18] C. Sekine, N. Konya, M. Minai, K. Fujisawa. *Liq. Cryst.*, **28**, 1361 (2001).
[19] C. Sekine, M. Ishitobi, K. Iwakura, M. Minai, K. Fujisawa. *Liq. Cryst.*, **29**, 355 (2002).
[20] C. Viney, D.J. Brown, C.M. Dannels, R.J. Twieg. *Liq. Cryst.*, **13**, 95 (1993).
[21] Y. Xu, Y. Hu, Q. Chen, J. Wen. *J. Mater. Chem.*, **5**, 219 (1995).
[22] R.J. Twieg, V. Chu, C. Nguyen, C.M. Dannels, C. Viney. *Liq. Cryst.*, **20**, 287 (1996).

[23] S.T. Wu, C.S. Hsu, Y.Y. Chuang. *Jap. J. appl. Phys.*, **38**, L286 (1999).
[24] O. Catanescu, L.C. Chien. *Liq. Cryst.*, **33**, 115 (2006).
[25] C.S. Hsu, K.F. Shyu, Y.Y. Chuang. *Liq. Cryst.*, **27**, 283 (2000).
[26] S.T. Wu, C.S. Hsu, K.F. Shyu. *Jap. J. appl. Phys. Lett.*, **74**, 344 (1999).
[27] S.T. Wu, C.S. Hsu, Y.Y. Chuang. *Jap. J. appl. Phys.*, **39**, L38 (1999).
[28] Y.H. Yao, L.R. Kung, S.W. Chang, C.S. Hsu. *Liq. Cryst.*, **33**, 33 (2006).
[29] H. Li, J. Wen. *Liq. Cryst.*, **33**, 1127 (2006).
[30] D.J. Spells, C. Lindsey, L.R. Dalton, S.T. Wu. *Liq. Cryst.*, **29**, 1529 (2002).